Laser-assisted inelastic electron-atom collisions

P. Francken and Y. Attaourti
Physique Théorique, Faculté des Sciences, Université Libre de Bruxelles (CP 227), Brussels, Belgium

C. J. Joachain
Physique Théorique, Faculté des Sciences, Université Libre de Bruxelles (CP 227), Brussels, Belgium and Institut de Physique Corpusculaire, Université de Louvain, Louvain-la-Neuve, Belgium

(Received 15 March 1988)

We study the inelastic scattering, accompanied by the transfer of L photons, of fast electrons by hydrogen and helium atoms in the presence of a laser field. A detailed analysis is made of the excitation of the $n=2$ and $n=3$ states of atomic hydrogen, and of the $1\,^1S-2\,^1S$ and $1\,^1S-2\,^1P$ transitions in helium. It is shown that the "dressing" effect due to the dipole distortion of the target by the laser field produces important modifications of the cross sections at small momentum transfers for S-S and S-D transitions. However, this dressing effect is reduced in the case of S-P transitions. Our results exhibit qualitative differences from the case of laser-assisted elastic collisions; this is mainly due to the possibility of intermediate resonances in the laser-atom interaction during the collision event.

I. INTRODUCTION

One of the most delicate aspects of the study of laser-assisted collisions consists in providing an adequate description of the target states in the presence of the laser field. This problem is particularly acute when strong fields are considered, or when the laser frequency is nearly resonant with an atomic transition. In three recent papers[1-3] a treatment of laser-assisted electron-atom collisions has been proposed, which is based on first-order time-dependent perturbation theory in the laser-atom interaction, while the laser-projectile interaction is treated nonperturbatively. This allows consideration of strong laser fields, provided that the electric field strengths $\mathcal{E}_0$ remain small with respect to the atomic unit of field strength, namely, $\mathcal{E}_0 \ll 5\times 10^9$ V cm^{-1}. The method also applies to all laser frequencies; however, in those cases where the laser photon energy is close to the energy of an atomic transition, limitations are imposed on the laser intensity. The method has already been applied to analyze laser-assisted elastic electron-hydrogen[1-3] and electron-helium[1,3] collisions.

In the present article we want to provide a generalization of our previous results to the case of laser-assisted excitation collisions. Such excitation processes have already been investigated by several authors,[4-7] mainly in the perturbative (weak-field) limit. As in the elastic case,[2] a comparison between the perturbative approach and the present nonperturbative treatment will be made. In what follows, the incident electron energy will be assumed to be high so that all calculations can be performed in the first Born approximation and exchange effects can be safely neglected.

II. THEORY

A. General method

Following our previous work, we assume the laser field to be monochromatic, linearly polarized, and spatially homogeneous. Working in the Coulomb gauge we have for the electric field and the vector potential $\mathcal{E}(t)=\mathcal{E}_0\sin\omega t$ and $\mathbf{A}(t)=\mathbf{A}_0\cos\omega t$ with $\mathbf{A}_0=c\mathcal{E}_0/\omega$. The wave function of the incident "unbound" electron embedded in that field is then given by the Volkov wave

$$\chi_{\mathbf{k}}(\mathbf{r}_0,t)=(2\pi)^{-3/2}\exp[i(\mathbf{k}\cdot\mathbf{r}_0-\mathbf{k}\cdot\boldsymbol{\alpha}_0\sin\omega t-E_k t/\hbar)]\ , \tag{1}$$

where $\mathbf{r}_0$ is the projectile coordinate, $\mathbf{k}$ denotes the electron wave vector, $E_k=\hbar^2k^2/2m$ is its kinetic energy, and $\boldsymbol{\alpha}_0=e\mathcal{E}_0/m\omega^2$. On the other hand, the "dressed" wave functions of the atomic target in the laser field are obtained, by using first-order time-dependent perturbation theory, as[8]

$$\Phi_n(X,t)=\exp(-iw_n t/\hbar)\exp(-i\mathbf{a}\cdot\mathbf{R})\left[\psi_n(X)-\sin\omega t\sum_{n'}\frac{\omega_{n',n}M_{n',n}}{\hbar(\omega_{n',n}^2-\omega^2)}\psi_{n'}(X)-i\cos\omega t\sum_{n'}\frac{\omega M_{n',n}}{\hbar(\omega_{n',n}^2-\omega^2)}\psi_{n'}(X)\right]\ , \tag{2}$$

where X denotes the ensemble of target coordinates, ψ_n is a target state of energy w_n in the absence of the external field, and $\omega_{n',n}$ is the Bohr frequency $\omega_{n',n}=(w_{n'}-w_n)/\hbar$. Furthermore, we have defined $\mathbf{a}=e\mathbf{A}/\hbar c$ and

$$M_{n',n}=M_{n,n'}^*=\mathcal{E}_0\cdot\langle\psi_{n'}\,|\,e\mathbf{R}\,|\,\psi_n\rangle\ , \tag{3}$$

where $\mathbf{R}=\sum_{j=1}^{Z}\mathbf{r}_j$ is the sum of all target coordinates, Z being the atomic number of the atom. In Eq. (2) the sum-

mation includes an integration over the continuum states.

The S-matrix element for inelastic scattering from the ground state to a final state of energy w_f, in the direct channel, in the presence of the laser field and in first Born approximation is then given in atomic units by

$$S_{f,0}^{\mathrm{B1}} = -i\int_{-\infty}^{+\infty} dt \langle \chi_{\mathbf{k}_f}(\mathbf{r}_0,t)\Phi_f(X,t) \mid V_d(\mathbf{r}_0,X) \mid \times \chi_{\mathbf{k}_i}(\mathbf{r}_0,t)\Phi_0(X,t)\rangle \ , \tag{4}$$

where

$$V_d(\mathbf{r}_0,X) = -\frac{Z}{r_0} + \sum_{j=1}^{Z} \frac{1}{r_{0j}} \tag{5}$$

is the direct interaction potential, with $r_{0j} = |\mathbf{r}_0 - \mathbf{r}_j|$. After integration on the time variable we have

$$S_{f,0}^{\mathrm{B1}} = (2\pi)^{-1} i \sum_{L=-\infty}^{+\infty} \delta(E_{k_f} - E_{k_i} + \omega_{f,0} - L\omega) f_{f,0}^{\mathrm{B1},L} \ . \tag{6}$$

Here $f_{f,0}^{\mathrm{B1},L}$ is the first-Born approximation to the inelastic scattering amplitude with the transfer of L photons, which can be written as

$$f_{f,0}^{\mathrm{B1},L} = J_L(\Delta\cdot\alpha_0) f_{f,0}^{\mathrm{B1}}(\Delta) - iJ_L'(\Delta\cdot\alpha_0)\left[\sum_{n'} \frac{\omega_{n',f} M_{f,n'}}{\omega_{n',f}^2 - \omega^2} f_{n',0}^{\mathrm{B1}}(\Delta) + \sum_{n'} \frac{\omega_{n',0} M_{n',0}}{\omega_{n',0}^2 - \omega^2} f_{f,n'}^{\mathrm{B1}}(\Delta)\right]$$

$$-iL\frac{J_L(\Delta\cdot\alpha_0)}{\Delta\cdot\alpha_0}\left[\sum_{n'} \frac{\omega M_{f,n'}}{\omega_{n',f}^2 - \omega^2} f_{n',0}^{\mathrm{B1}}(\Delta) - \sum_{n'} \frac{\omega M_{n',0}}{\omega_{n',0}^2 - \omega^2} f_{f,n'}^{\mathrm{B1}}(\Delta)\right] . \tag{7}$$

In this formula $\Delta = \mathbf{k}_i - \mathbf{k}_f$ is the momentum transfer, J_L is an ordinary Bessel function of order L, and J_L' is its first derivative. Moreover, $f_{f,0}^{\mathrm{B1}}(\Delta)$, $f_{n',0}^{\mathrm{B1}}(\Delta)$, and $f_{f,n'}^{\mathrm{B1}}(\Delta)$ are the first Born amplitudes corresponding to the scattering events $0\to f$, $0\to n'$, and $n'\to f$ in the absence of the laser field.

The first term on the right-hand side of Eq. (7), which we will call "electronic," corresponds to the interaction of the laser field with the incident electron only. The following ones, called "atomic," are due to dressing effects. It should be noted that the sums over intermediate states appearing in that expression can be divided in two classes because of the selection rules arising from the matrix elements $M_{n',n}$. Indeed, the first sum in each large parentheses only involves intermediate states with angular momentum $l' = l \pm 1$, where we denote by l the angular momentum of the final state. On the other hand, the second sum in each large parentheses only involves intermediate p states.

The first Born differential cross sections corresponding to the various multiphoton processes are given by

$$\frac{d\sigma_{0\to f}^{\mathrm{B1},L}}{d\Omega} = \frac{k_f}{k_i} |f_{f,0}^{\mathrm{B1},L}|^2 \ . \tag{8}$$

It is worth stressing that in contrast to the case of elastic collisions, the atomic transition energies $\omega_{n',f}$ corresponding to transitions involving the final state can be of the same order of magnitude as the photon energy, when considering standard lasers operating in the ir-vuv range. Consequently, the closure approximation proposed in Refs. 1–3 for elastic collisions has to be adequately modified in the case of inelastic collision processes in the presence of a laser field.

B. Atomic hydrogen target

Let us now focus our attention on laser-assisted electron-atomic hydrogen excitation. These processes are of particular interest since an exact calculation of the first Born scattering amplitude given by Eq. (7) can be performed. This constitutes an important advantage in the context of inelastic collisions where, in contrast to the elastic case, the simple closure approximation is inadequate. Moreover, the availability of such exact first-Born atomic hydrogen results will allow us to check the validity of further approximations which must be made when treating the case of complex atoms.

The main problem in evaluating Eq. (7) consists in obtaining general expressions for the matrix elements $f_{n,n'}^{\mathrm{B1}}(\Delta)$ and $M_{n,n'}$, both in the case of bound-bound and bound-free transitions. Let us first consider the case of the matrix elements $M_{n,n'}$; these can be expressed in terms of their spherical components

$$M_{n,n'} = \sum_{q=0,\pm1} \hat{\varepsilon}_q^* M_{n,n'}^q \ . \tag{9}$$

Since it is convenient in the calculations to take the quantization axis along the momentum transfer Δ, the spherical components of the polarization vector $\hat{\varepsilon}$ (the unit vector along $\mathcal{E}_0$) are now given by

$$\hat{\varepsilon}_0 = \Delta^{-1}[k_f\cos(\theta_\gamma - \theta) - k_i\cos\theta_\gamma] \ , \tag{10a}$$

$$\hat{\varepsilon}_1 = \hat{\varepsilon}_{-1} = \frac{-i}{\sqrt{2}}\Delta^{-1}[\sin\theta_\gamma(k_f\cos\theta - k_i) - k_f\cos\theta_\gamma\sin\theta] \ , \tag{10b}$$

where θ and θ_γ denote, respectively, the scattering angle and the angle between the polarization vector $\hat{\varepsilon}$ and the incident momentum $\mathbf{k}_i$.

In the case where the intermediate states n' are hydrogen bound states, which we shall now denote by their three quantum numbers $n'l'm'$, the quantities $M_{nlm,n'l'm'}^q$ are readily evaluated by using the expression of the hydrogen bound state wave functions in terms of confluent hypergeometric functions. We obtain

$$M^q_{nlm,n'l'm'}=\mathcal{E}_0(-1)^m\frac{2^{l+l'+2}}{n^{l+2}n'^{l'+2}}\frac{[(2l+1)(2l'+1)]^{1/2}}{(2l+1)!(2l'+1)!}\left[\frac{(n+l)!(n'+l')!}{(n-l-1)!(n'-l'-1)!}\right]^{1/2}\begin{bmatrix}1 & l' & l\\ 0 & 0 & 0\end{bmatrix}\begin{bmatrix}1 & l' & l\\ q & m' & -m\end{bmatrix}$$

$$\times\sum_{\mu=0}^{n-l-1}\frac{(l+1-n)_\mu}{(2l+2)_\mu\mu!}\left[\frac{2}{n}\right]^\mu\sum_{\mu'=0}^{n'-l'-1}\frac{(l'+1-n')_{\mu'}}{(2l'+2)_{\mu'}\mu'!}\left[\frac{2}{n'}\right]^{\mu'}\frac{(l+l'+\mu+\mu'+3)!}{\alpha^{l+l'+\mu+\mu'+4}}\ , \tag{11}$$

where we have defined $\alpha=1/n+1/n'$.

Let us now consider intermediate states belonging to the continuous part of the spectrum. Denoting these states by $p'l'm'$ and using a continuum wave function normalized with respect to the energy, one can easily obtain $(0\le p'\le\infty)$

$$M^q_{nlm,p'l'm'}=\mathcal{E}_0(-1)^m\frac{2^{l+l'+2}}{n^{l+2}}\frac{1}{(2l+1)!(2l'+1)!}\left[\frac{(2l+1)(2l'+1)(n+l)!}{(n-l-1)!}\right]^{1/2}$$

$$\times\prod_{s=0}^{l'}(p'^2s^2+1)^{1/2}(1-e^{-2\pi/p'})^{-1/2}\begin{bmatrix}1 & l' & l\\ 0 & 0 & 0\end{bmatrix}\begin{bmatrix}1 & l' & l\\ q & m' & -m\end{bmatrix}$$

$$\times\sum_{\mu=0}^{n-l-1}\frac{(l+1-n)_\mu}{(2l+2)_\mu\mu!}\left[\frac{2}{n}\right]^\mu\frac{(l+l'+\mu+3)!}{\left[\frac{1}{n}-ip'\right]^{l+l'+\mu+4}}$$

$$\times{}_2F_1\left[l'+1-i/p',l+l'+\mu+4,2l'+2,\frac{-2ip'}{1/n-ip'}\right]\ . \tag{12}$$

Note that because of the selection rule $l'=l\pm1$, the last hypergeometric function can always be transformed into a polynomial of finite degree.

The field-free first-Born scattering amplitudes $f^{\mathrm{B1}}_{n,n'}(\Delta)$ are readily evaluated in the following way. Using the Bethe formula, we have

$$f^{\mathrm{B1}}_{n,n'}(\Delta)=-2\Delta^{-2}\langle n\mid e^{i\Delta\cdot\mathbf{r}_1}-1\mid n'\rangle\ . \tag{13}$$

For an intermediate bound state with quantum numbers n',l',m' we find that

$$\langle nlm\mid e^{i\Delta\cdot\mathbf{r}_1}-1\mid n'l'm'\rangle$$

$$=(-1)^m\frac{2^{l+l'+2}}{n^{l+2}n'^{l'+2}}\frac{[(2l+1)(2l'+1)]^{1/2}}{(2l+1)!(2l'+1)!}\left[\frac{(n+l)!(n'+l')!}{(n-l-1)!(n'-l'-1)!}\right]^{1/2}$$

$$\times\sum_{\lambda=|l-l'|}^{l+l'}i^\lambda(2\lambda+1)\begin{bmatrix}\lambda & l' & l\\ 0 & 0 & 0\end{bmatrix}\begin{bmatrix}\lambda & l' & l\\ 0 & m' & m\end{bmatrix}\frac{\sqrt{\pi}\Delta^\lambda}{2^{\lambda+1}\Gamma(\lambda+3/2)}$$

$$\times\sum_{\mu=0}^{n-l-1}\sum_{\mu'=0}^{n'-l'-1}\frac{(l+1-n)_\mu(l'+1-n')_{\mu'}}{(2l+2)_\mu(2l'+2)_{\mu'}\mu!\mu'!}\left[\frac{2}{n}\right]^\mu\left[\frac{2}{n'}\right]^{\mu'}\frac{(\mu+\mu'+l+l'+\lambda+3)!}{\alpha^{\mu+\mu'+l+l'+\lambda+4}}$$

$$\times{}_2F_1\left[\frac{\mu+\mu'+l+l'+\lambda+3}{2},\frac{\mu+\mu'+l+l'+\lambda+4}{2},\lambda+\frac{3}{2},-\Delta^2/\alpha^2\right]$$

$$-\delta_{n,n'}\delta_{l,l'}\delta_{m,m'}\ . \tag{14}$$

Finally, in the case of an intermediate state lying in the continuous spectrum we obtain

$$
\begin{aligned}
&\langle nlm \mid e^{i\Delta\cdot r_1}-1 \mid p'l'm'\rangle \\
&\quad=(-1)^m \frac{2^{l+l'+2}}{n^{l+2}} \frac{[(2l+1)(2l'+1)]^{1/2}}{(2l+1)!(2l'+1)!} \left[\frac{(n+l)!}{(n-l-1)!}\right]^{1/2} \\
&\qquad\times \prod_{s=0}^{l} (p'^2 s^2+1)^{1/2}(1-e^{-2\pi/p'})^{-1/2} \\
&\qquad\quad\times \sum_{\lambda=|l-l'|}^{l+l'} i^{\lambda}(2\lambda+1) \begin{pmatrix} \lambda & l' & l \\ 0 & 0 & 0 \end{pmatrix} \begin{pmatrix} \lambda & l' & l \\ 0 & m' & -m \end{pmatrix} \\
&\qquad\qquad\times \sum_{\mu=0}^{n-l-1} \frac{(l+1-n)_\mu}{(2l+2)_\mu \mu!} \left[\frac{2}{n}\right]^{\mu} \frac{1}{2\Delta} \\
&\qquad\qquad\quad\times \sum_{\sigma=0}^{\lambda} \frac{(\lambda+\sigma)!\, i^{\sigma-\lambda-1}}{\sigma!(\lambda-\sigma)!(2\Delta)^{\sigma}} \Gamma(l+l'-\sigma+\mu+2) \\
&\qquad\qquad\qquad\times \left[\left[\frac{1}{n}+ip'-i\Delta\right]^{-(l+l'-\sigma+\mu+2)} \right. \\
&\qquad\qquad\qquad\quad\times {}_2F_1\left[l+1+i/p', l+l'-\sigma+\mu+2, 2l'+2, \frac{2ip'}{1/n+ip'-i\Delta}\right] \\
&\qquad\qquad\qquad\quad+(-1)^{\sigma-\lambda-1}\left[\frac{1}{n}+ip'+i\Delta\right]^{-(l+l'-\sigma+\mu+2)} \\
&\qquad\qquad\qquad\quad\left.\times {}_2F_1\left[l+1+i/p', l+l'-\sigma+\mu+2, 2l'+2, \frac{2ip'}{1/n+ip'+i\Delta}\right]\right], \qquad (15)
\end{aligned}
$$

where we have used a well-known representation of the Bessel functions of half-integer order in terms of inverse powers of the argument.[9] Note that since continuum wave functions only appear as intermediate states, we have omitted in Eqs. (12) and (15) the Coulomb phase of these wave functions.

C. Helium target

In contrast with the case of atomic hydrogen, an exact evaluation of Eq. (7) is not possible since no general, accurate wave functions are known for all excited states of helium. On the other hand, although the closure approximation could be used to evaluate the terms containing denominators of the type $\omega_{n',0}^2-\omega^2$ on the right-hand side of Eq. (7), we know that this method would fail for the remaining terms. However, we will now show that the problem can be circumvented at the price of a slightly less accurate treatment than in the case of atomic hydrogen. Indeed, one can expect in general that only the few intermediate states with lower energy contribute significantly, provided the laser frequency remains small enough. As will be shown below this can actually be proved for a hydrogen target, and it is quite reasonable to assume that the same situation remains true for helium. This suggests the possibility of approximating the "exact" first-Born scattering amplitude given by Eq. (7) by including exactly only those intermediate states which contribute significantly to the sum, while using the closure approximation to account for the other states. This yields the following approximation of the scattering amplitude:

$$
\begin{aligned}
\tilde{f}_{f,0}^{\mathrm{BI},L} &= J_L(\Delta\cdot\alpha_0) f_{f,0}^{\mathrm{BI}}(\Delta) \\
&\quad -\frac{2}{\Delta^2}[\mathcal{E}_0\cdot\nabla_\Delta\langle\psi_f(\mathbf{r}_1,\mathbf{r}_2)\mid e^{i\Delta\cdot r_1}+e^{i\Delta\cdot r_2}-2\mid\psi_0(r_1,r_2)\rangle+2iM_{f,0}-2i\mathcal{E}_0\cdot\langle\psi_f(\mathbf{r}_1,\mathbf{r}_2)\mid \mathbf{r}_1 e^{i\Delta\cdot r_2}\mid\psi_0(\mathbf{r}_1,\mathbf{r}_2)\rangle] \\
&\qquad\times\left[J_L'(\Delta\cdot\alpha_0)\left[\frac{\bar{\omega}_f}{\bar{\omega}_f^2-\omega^2}+\frac{\bar{\omega}_0}{\bar{\omega}_0^2-\omega^2}\right]-L\frac{J_L(\Delta\cdot\alpha_0)}{\Delta\cdot\alpha_0}\left[\frac{\omega}{\bar{\omega}_f^2-\omega^2}-\frac{\omega}{\bar{\omega}_0^2-\omega^2}\right]\right] \\
&\qquad -iJ_L'(\Delta\cdot\alpha_0)\sum_m M_{f,m} f_{m,0}^{\mathrm{BI}}(\Delta)\left[\frac{\omega_{m,f}}{\omega_{m,f}^2-\omega^2}-\frac{\bar{\omega}_f}{\bar{\omega}_f^2-\omega^2}\right] \\
&\qquad +iL\frac{J_L(\Delta\cdot\alpha_0)}{\Delta\cdot\alpha_0}\sum_m M_{f,m} f_{m,0}^{\mathrm{BI}}(\Delta)\left[\frac{\omega}{\omega_{m,f}^2-\omega^2}-\frac{\omega}{\bar{\omega}_f^2-\omega^2}\right], \qquad (16)
\end{aligned}
$$

where $\bar{\omega}_0$ is the average difference between the energy of an intermediate state and that of the ground state (i.e., the average excitation energy), while $\bar{\omega}_f$ is the average difference between the energy of an intermediate state and that of the final state. For $\bar{\omega}_0$ we have chosen the value 1.15 a.u., which gives the correct dipole polarizability of the helium ground state, $\bar{\alpha}=1.38$. The choice of $\bar{\omega}_f$ will be discussed below. In writing down Eq. (16) we have only considered the case of final and intermediate singlet states, since exchange effects (which are small at high energies) are not included in our treatment. The sum over m appearing in Eq. (16) now involves only those intermediate states which we treat exactly. As a rule, we shall always include at least all the intermediate states with principal quantum number $n \leq 3$.

Let us first consider the electron impact excitation of the $2\,^1S$ state, with the transfer of L photons. For the ground state we have used the wave function[10]

$$\psi_{1\,^1S}(r_1,r_2)=\phi_0(r_1)\phi_0(r_2)\ , \tag{17}$$

where the orbital $\phi_0(r)$ is given by

$$\phi_0(r)=(4\pi)^{-1/2}(Ae^{-\alpha r}+Be^{-\beta r})\ , \tag{18}$$

with $A=2.605\,05$, $B=2.081\,44$, $\alpha=1.41$, and $\beta=2.61$. For the $2\,^1S$ state we have chosen the wave function[11]

$$\psi_{2\,^1S}(r_1,r_2)=C[u_1(r_1)u_2(r_2)+u_1(r_2)u_2(r_1)]\ , \tag{19}$$

where

$$u_1(r)=(4\pi)^{-1/2}Me^{-2r} \tag{20}$$

and

$$u_2(r)=(4\pi)^{-1/2}N(e^{-\tau_1 r}-Sre^{-\tau_2 r})\ , \tag{21}$$

the values of the parameters being $C=0.705\,226$, $M=5.656\,854$, $N=0.619\,280$, $\tau_1=0.865$, $\tau_2=0.522$, and $S=0.432\,784$.

Because in the case of the excitation of the $2\,^1S$ state we have only to consider ^1P intermediate states in Eq. (16), it is a simple matter to include all (simply) excited states of this kind, which we represent by expressions of the form

$$\psi_{n\,^1P}(\mathbf{r}_1,\mathbf{r}_2)=\frac{1}{\sqrt{2}}[\psi_{1s}(Z_i,r_1)\psi_{npm}(Z_0,\mathbf{r}_2) +\psi_{1s}(Z_i,r_2)\psi_{npm}(Z_0,\mathbf{r}_1)]\ , \tag{22}$$

where ψ_{1s} and ψ_{npm} are hydrogenic wave functions corresponding to $1s$ and npm states with effective charges $Z_i=2$ and $Z_0=1$, respectively, and the index n can take both discrete and continuum values. Doubly excited states are not taken into account by this method. However, their contribution can be estimated by using the closure method (see Appendix A) and is found to be small.

Let us now consider the excitation of the $2\,^1P$ state. Since we want to include exactly in Eq. (16) all intermediate states with principal quantum number $n \leq 3$, we also need in the present case the wave functions of the $3\,^1S$ and $3\,^1D$ states. For the $3\,^1S$ state we have constructed a wave function of the form

$$\psi_{3\,^1S}(r_1,r_2)=\tilde{C}[u_1(r_1)u_3(r_2)+u_1(r_2)u_3(r_1)]\ , \tag{23}$$

where $u_1(r)$ is given by Eq. (20),

$$u_3(r)=(4\pi)^{-1/2}\tilde{N}[e^{-\sigma_1 r}-Pre^{-\sigma_2 r}+Qr^2e^{-\sigma_3 r}] \tag{24}$$

and the values of the parameters are $\tilde{C}=0.512\,410$, $\tilde{N}=0.456\,615$, $\sigma_1=0.331$, $\sigma_2=0.464$, $\sigma_3=0.330$, $P=0.932\,435$, and $Q=0.038\,820$. This wave function, which is orthogonal to the $1\,^1S$ wave function (17) and the $2\,^1S$ wave function (19), gives the accurate value -2.0606 a.u. for the energy of the $3\,^1S$ state. For the $3\,^1D$ state, we have used a wave function of the type

$$\psi_{3\,^1D}(\mathbf{r}_1,\mathbf{r}_2)=\frac{1}{\sqrt{2}}[\psi_{1s}(Z_i,r_1)\psi_{3dm}(Z_0,\mathbf{r}_2) +\psi_{1s}(Z_i,r_2)\psi_{3dm}(Z_0,\mathbf{r}_1)] \tag{25}$$

where $\psi_{1s}(Z_i,r)$ and $\psi_{3dm}(Z_0,\mathbf{r})$ are hydrogenic wave functions corresponding to the effective charges $Z_i=2$ and $Z_0=1$, respectively.

III. RESULTS AND DISCUSSION

A. Atomic hydrogen target

Before presenting the results of our calculations, we want to make a remark concerning the domain of validity of the treatment used for taking into account the laser-atom interaction. Indeed, since the main criterion for the validity of our perturbative treatment is that the interaction be nonresonant, the possibility that the laser frequency matches the frequency of an atomic transition in the case of a laser-assisted excitation collision process induces new limitations for the values of the intensity which can be considered. Let us denote by (n,n') any pair of states which can be connected by an intermediate radiative transition during the scattering event. Hence, a quantitative estimate of these limiting values of the field intensity can be obtained by the requirement

$$|M_{n,n'}| \ll |\omega_{n,n'}-\omega|\ , \tag{26}$$

where the quantity $M_{n,n'}$ is defined by Eq. (3) and plays the role of a coupling parameter. We could ask, for ex-

TABLE I. Maximum values of the electric field strength (in V cm^{-1}) allowed by our perturbative approach for various dipole transitions in atomic hydrogen and two typical laser frequencies. The numbers in brackets indicate powers of ten.

	$\hbar\omega=0.117$ eV			
	$1s$	$2s$	$3s$	$4s$
$2p$	2.559[8]	7.373[5]	6.183[7]	2.084[8]
$3p$	7.587[8]	1.893[7]	3.010[5]	7.291[6]
$4p$	1.358[9]	6.213[7]	3.257[6]	1.649[5]
	$\hbar\omega=1.17$ eV			
	$1s$	$2s$	$3s$	$4s$
$2p$	2.292[8]	7.373[6]	2.508[7]	1.182[8]
$3p$	6.919[8]	7.680[6]	3.010[6]	6.819[6]
$4p$	1.245[9]	3.524[7]	3.047[6]	1.649[6]

ample, that the detuning remains always more than ten times greater than the term on the left-hand side of Eq. (26). The maximum values allowed for the electric field strength under this condition are displayed in Table I for various dipole transitions and for two typical laser frequencies. In the case of a final state with principal quantum number $n=2$, for instance, the condition (26) is satisfied for the frequency corresponding to a Nd:YAG yttrium aluminum garnet laser, namely, $\hbar\omega=1.17$ eV, provided that $\mathcal{E}_0<10^6$ V cm^{-1}. For final states corresponding to $n=3$, on the other hand, a high-intensity Nd:YAG laser can certainly not be considered since it would be strongly resonant with the intermediate transition between the $n=6$ and $n=3$ levels ($\hbar\omega_{6,3}=1.33$ eV). Nevertheless, an infrared laser, for instance a CO_2 laser ($\hbar\omega=0.117$ eV) can be used without matching any atomic transition. In that case, Eq. (26) implies that the electric field strength $\mathcal{E}_0$ should not be higher than 2×10^5 V cm^{-1} (see Table I).

In Figs. 1–3 we give the differential cross sections corresponding to the excitation of the $2s$, $3s$, and $3d$ states with the absorption of one photon ($L=1$), as a function

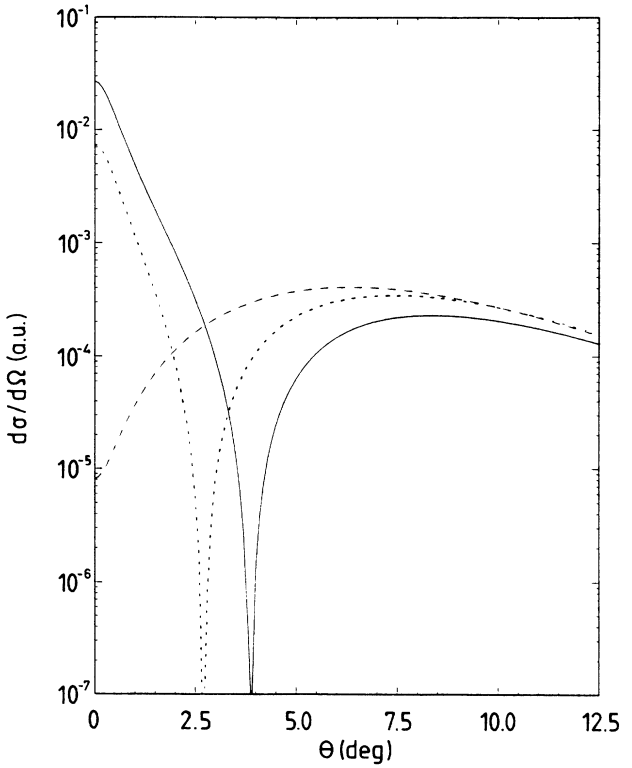

FIG. 1. First-Born differential cross section corresponding to the electron-impact excitation of the $2s$ state of atomic hydrogen with absorption of one photon ($L=1$). The incident electron energy is $E_i=500$ eV, the laser photon energy is $\hbar\omega=1.17$ eV, and the electric field strength is $\mathcal{E}_0=10^6$ V cm^{-1}. The polarization vector of the field is chosen to be parallel to the momentum transfer Δ. Solid line, full calculation using Eq. (7); dashed line, electronic result obtained by neglecting the dressing of the target; dotted line, calculation of Eq. (7) within the closure approximation.

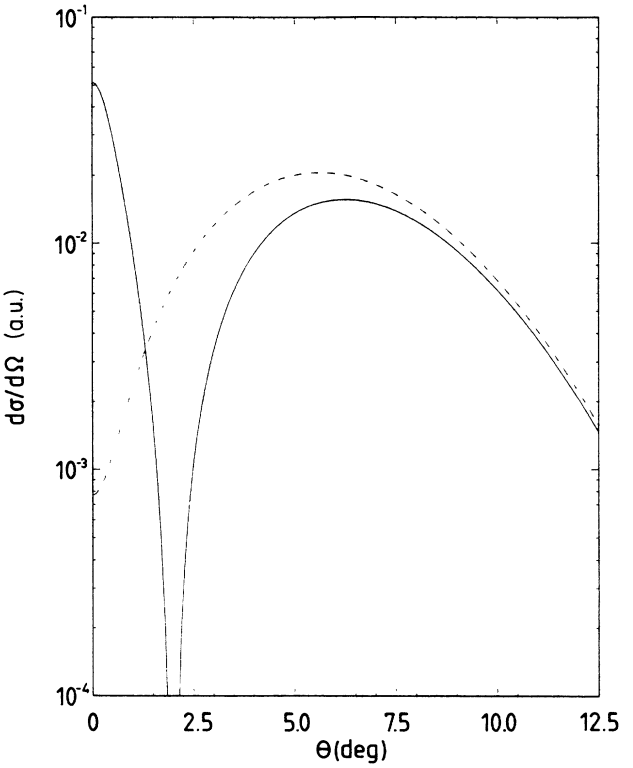

FIG. 2. Same as Fig. 1 but for the excitation of the $3s$ state of atomic hydrogen, a laser photon energy $\hbar\omega=0.117$ eV, and an electric field strength $\mathcal{E}_0=2\times10^5$ V cm^{-1}.

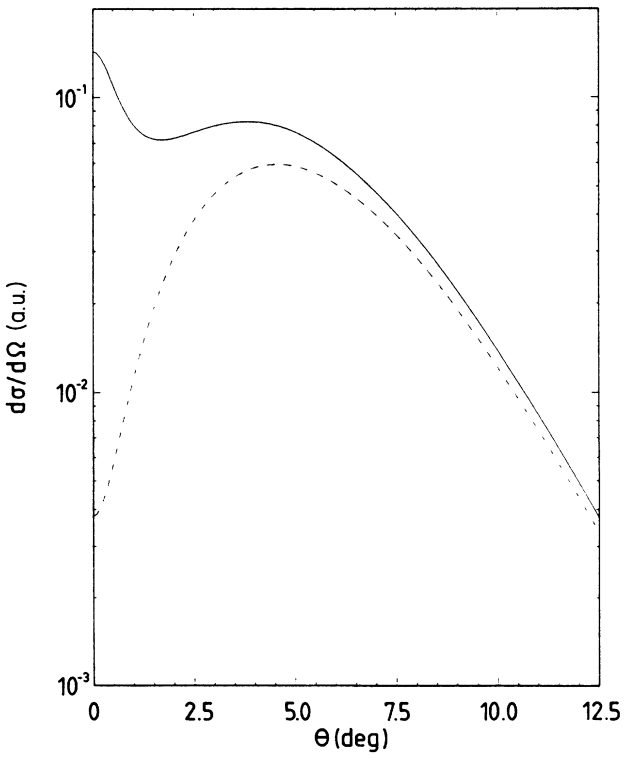

FIG. 3. Same as Fig. 2 but for the excitation of the $3d$ state of atomic hydrogen.

TABLE II. Contribution (in percent) of the various intermediate states to the dressing term in Eq. (7), in the case of an atomic hydrogen target and for a fixed scattering angle $\theta=10°$. The incident electron energy, the laser photon energy, and the electric field strength are chosen as in Figs. 1–3.

	$\hbar\omega=1.17$ eV, $\mathcal{E}_0=10^6$ V cm^{-1}		$\hbar\omega=0.117$ eV, $\mathcal{E}_0=2\times10^5$ V cm^{-1}		
	Final state				
Intermediate state	$2s$	$2p$	$3s$	$3p$	$3d$
$1s$		5.16		0.22	
$2s$		64.85		3.45	
$3s$		2.26		64.49	
$4s$		0.48		2.27	
$2p$	79.71	15.25	1.30	0.18	8.47
$3p$	9.86	0.47	86.71	0.56	86.75
$4p$	2.21	0.17	6.99	0.01	2.10
$3d$		4.77		21.30	
$4d$		1.06		3.46	
$4f$					0.91

of the scattering angle θ and for an incident energy $E_i=500$ eV. We are working in a geometry in which the polarization vector $\hat{\boldsymbol{\varepsilon}}$ of the field (which is along $\boldsymbol{\mathcal{E}}_0$ for the case of linear polarization considered here) is parallel to the momentum transfer $\boldsymbol{\Delta}$. According to our previous discussion, the laser frequency and electric field strength will be taken to be 1.17 eV and 10^6 V cm^{-1}, respectively, in the case of a final $2s$ state, and 0.117 eV and 2×10^5 V cm^{-1}, respectively, in the case of a final $3s$ or $3d$ state.

In Fig. 1 we show the cross section corresponding to the $1s\rightarrow2s$ excitation process. The complete result, obtained by using the scattering amplitude (7), is compared to the "electronic" cross section in which dressing effects are neglected. As in the case of elastic collisions,[1–3] dressing effects are seen to be dominant in the forward direction. This is due to the presence in the "atomic" term of S-P transition amplitudes which behave like Δ^{-1} for small Δ. Moreover, we notice a destructive interference between the electronic and atomic amplitudes near $\theta=3.8°$. The presence of such interferences is a general feature of $1s\rightarrow ns$ transitions in the case of inverse bremsstrahlung ($L>0$), provided that one considers low-frequency lasers [such that the laser frequency is less than the frequency corresponding to the lowest resonance appearing in Eq. (7)]. Also shown in Fig. 1 is the cross section obtained in the closure approximation by replacing in Eq. (7) $\omega_{n',0}$ by a mean value $\bar{\omega}=\frac{4}{9}$ a.u. and $\omega_{n',f}$ by 0 which is a reasonable choice since the final $2s$ state will be mainly coupled with the intermediate $2p$ state and both are energy degenerate. We stress that the discrepancy between the "exact" and the closure results increases when other mean values are taken for $\omega_{n',f}$. This confirms that the closure approximation is not reliable in the present context.

The results displayed in Fig. 2 correspond to the $1s\rightarrow3s$ transition and show a qualitatively similar behavior as in the case of the $1s\rightarrow2s$ process. However, the dressing effects are now less important, since the electric field strength is here reduced to 2×10^5 V cm^{-1}. In Fig. 3 it is seen that dressing effects are also dominant, at small scattering angles, in the case of the $1s\rightarrow3d$ transition. Moreover, we notice that in this case the interference between the atomic and electronic amplitudes is constructive; this is in contrast with the results obtained for $1s\rightarrow ns$ transitions. We do not show figures concerning $1s\rightarrow np$ transitions, since dressing effects are rather small in this case. Indeed the electronic s-p amplitude, which behaves like Δ^{-1} for small Δ, now dominates the cross section at small angles.

In Table II we give the contribution (in percent) of the various intermediate states to the dressing term in Eq. (7) for a fixed scattering angle $\theta=10°$; the other parameters are chosen as in the figures. It is seen that in every case only a few intermediate states contribute significantly to the sum, in agreement with our discussion preceding Eq. (16).

In Figs. 4 and 5, the frequency dependence of the cross sections is shown for $L=1$, $E_i=500$ eV, and a fixed scattering angle $\theta=5°$. Here we have developed the Bessel functions appearing in Eq. (7) to first order and we have normalized our cross sections to the mean laser intensity $I=c\mathcal{E}_0^2/8\pi$. Our results then reduce to first order ones (both in the laser-projectile and laser-atom interactions), and the electric field is assumed weak enough for first-order perturbation theory to hold even in the vicinity of atomic transition frequencies. Note that in this limit our results reduce to those obtained by Jetzke *et al.*,[6] in the same way as in the elastic case.[2]

Figures 4 and 5, showing abrupt changes in the vicinity of Bohr frequencies, indicate that the behavior of the cross sections with respect to the laser frequency strongly depends on the structure of the target. It is also interesting to note that the results are sensitive to the presence of those Bohr frequencies even far away from resonance. Another interesting feature is that, in the case of a final state with principal quantum number $n=2$, one does not observe peaks corresponding to virtual dipole transitions ending in the final state, while in the case of final states with $n=3$ only intermediate states with $n=2$ are seen to contribute to such resonant processes. This could seem

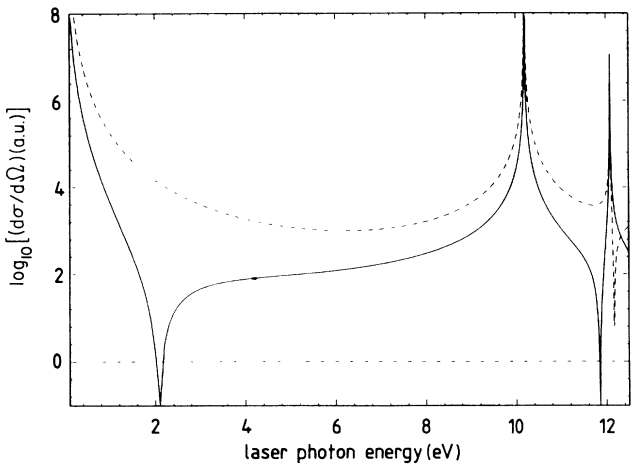

FIG. 4. Variation of $\log_{10}(d\sigma/d\Omega)$ as a function of the laser photon energy, for the electron-impact excitation of the $n=2$ states of atomic hydrogen in the presence of a laser field and in the case $L=1$. The incident electron energy is $E_i=500$ eV and the scattering angle is $\theta=5°$. The electric field $\mathcal{E}$ is assumed to be weak and is chosen to be parallel to the momentum transfer Δ. The cross sections have been normalized to the mean laser intensity $I=c\mathcal{E}_0^2/8\pi$. Solid line, excitation of the $2s$ state; dashed line, excitation of the $2p$ state.

rather surprising since our transition amplitude Eq. (7) presents poles corresponding to all radiative transitions between intermediate and final (as well as initial) states. However it can be shown quite generally (see Appendix B) that these intermediate resonances, when occurring in a transition between an intermediate state and the final state, "cancel out" to lowest order in the field in the case $L>0$ (absorption or inverse bremsstrahlung) except for intermediate states with lower energy than the final state.

Let us now turn to the case $L<0$ (emission or stimulated bremsstrahlung). Figure 6 shows that, in contrast to the case $L=+1$, the frequency dependence of the $1s\rightarrow 2s$ and $1s\rightarrow 2p$ cross sections, for $L=-1$, exhibits peaks corresponding to radiative transitions ending in the final state. The reason for this behavior is discussed in detail in Appendix B. However, it can readily be understood that since the atom interacts only once with the laser field in the weak-field limit considered here, a resonant transition between an intermediate state and the final state can only take place through the absorption of one photon if the intermediate state has a lower energy than the final state (that is, the atom gains energy). Conversely, that transition can only be resonant in the case of emission for an intermediate state having a higher energy than the final state. We also note that, even at higher field intensities, it is apparent from Eq. (7) that important asymetries between emission and absorption should be expected. This is because, under the substitution $L\rightarrow -L$, the term proportional to $J_L'(x)$ behaves like the "electronic" term, which is proportional to $J_L(x)$ [that is, it is multiplied by a factor $(-1)^L$] while the term proportional to $L\,J_L(x)/x$ (which did not appear in the elastic case[1-3]) is multiplied by a factor $(-1)^{L+1}$.

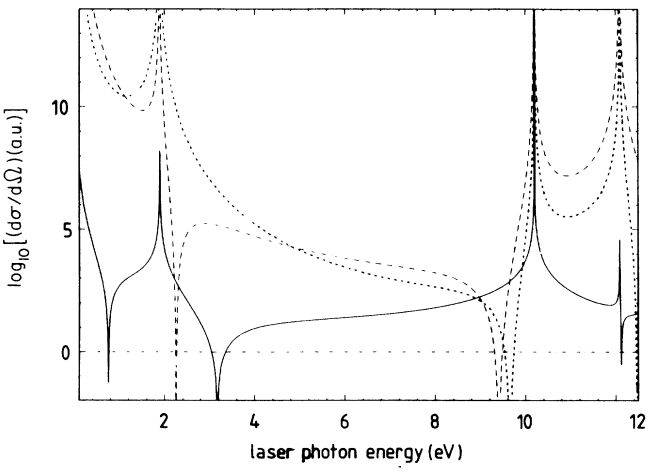

FIG. 5. Same as Fig. 4 but for the excitation of the $n=3$ states of atomic hydrogen. Solid line, excitation of $3s$ state; dashed line, excitation of the $3p$ state; dotted line, excitation of the $3d$ state.

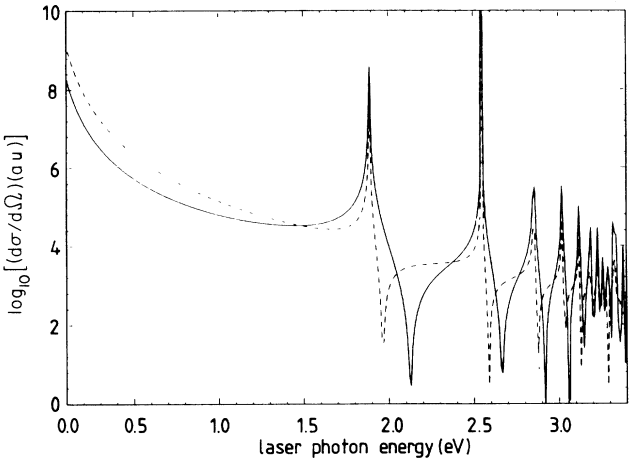

FIG. 6. Same as Fig. 4 but for the emission of one photon $(L=-1)$.

B. Helium target

We first display some results which clearly vindicate the validity of our method and confirm the discussion of Sec. II B. In Table III we give various results concerning the evaluation of the scattering amplitude, Eq. (7), in the case of a final $2\,^1S$ state and for one absorbed photon $(L=1)$. This evaluation has been performed in several ways: (a) by replacing $\omega_{n'f}$ by an average excitation energy (for all intermediate states, including the $2\,^1P$ and $3\,^1P$ ones) and performing the summation analytically by closure; (b) with the same average energy, but performing the summation numerically with the help of the wave functions (22); (c) by closure, but including exactly the $2\,^1P$ and $3\,^1P$ states with their correct energies, according to Eq. (16); (d) according to Eq. (16), but with explicit in-

TABLE III. Evaluation of the scattering amplitude, Eq. (7), in the case of the excitation of the $2\,^1S$ state of helium and for one absorbed photon ($L=1$), as a function of the average energy $\bar{\omega}_{2\,^1S}$. Column (a), analytical calculation in the closure approximation; column (b), numerical calculation in the closure approximation, using intermediate states described by Eq. (22); column (c), numerical calculation with the "exact" inclusion of the $2\,^1P$ and $3\,^1P$ intermediate states; column (d), numerical calculation with the exact inclusion of all simply excited intermediate states; column (e), evaluation of the contribution of doubly excited states. The numbers in brackets indicate powers of ten.

Average energy $\bar{\omega}_{2\,^1S}$	(a)	(b)	(c)	(d)	(e)
0.1	−9.627 681[−3]	−9.651 368[−3]	−6.639 757[−3]	−5.996 811[−3]	2.819 730[−4]
0.218	−9.967 787[−3]	−9.980 736[−3]	−6.036 013[−3]	−6.007 510[−3]	1.547 696[−4]
0.5	−1.018 200[−2]	−1.018 823[−2]	−5.655 717[−3]	−6.014 206[−3]	7.440 103[−5]
1.37	−1.030 406[−2]	−1.030 647[−2]	−5.438 981[−3]	−6.018 090[−3]	2.859 280[−5]

clusion of *all* simply excited intermediate states (up to numerical saturation); (e) finally, the contribution of doubly excited states, calculated as described in Appendix A, is also given in Table III.

From the analysis of these results, the following conclusions can be drawn. Firstly, it is seen that the closure result (a) always agrees with its counterpart (b): This proves that our choice for the wave functions of the intermediate states is adequate. Secondly, we see that the explicit inclusion of the $2\,^1P$ and $3\,^1P$ states (c) considerably affects the closure results (a): This confirms that our improvement of the latter is necessary. Thirdly, we remark that the explicit inclusion of two intermediate states (c) or more (d) yields very similar results. In particular, the best agreement is obtained for our "best value" $\bar{\omega}_{2\,^1S}=0.218$ a.u., which has been fitted for $\theta=0°$. Finally, the contribution of doubly excited states is seen to be small. In Table III the scattering angle is taken to be $\theta=5°$, the incident electron energy is $E_i=500$ eV, the electric field strength is $\mathcal{E}_0=10^6$ V cm^{-1} and we are working in the geometry in which $\mathcal{E}_0$ is parallel to the momentum transfer Δ. The photon energy corresponds

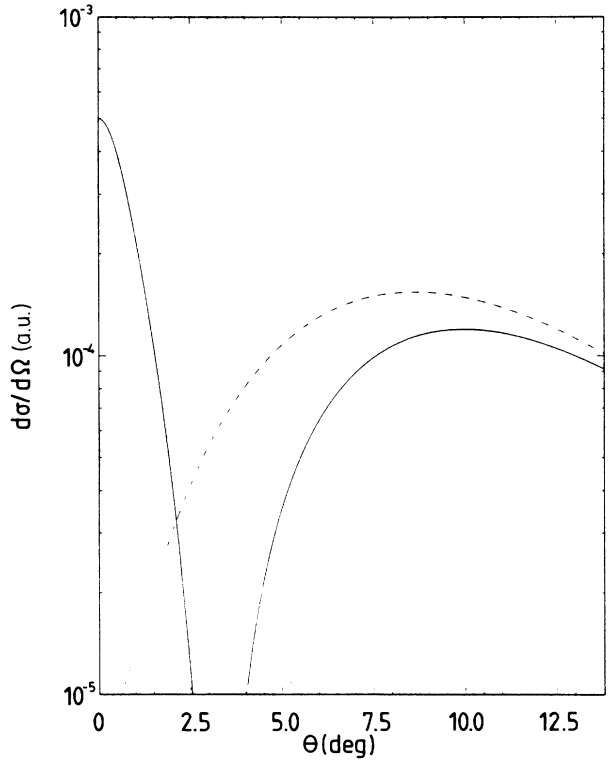

FIG. 7. First-Born differential cross section corresponding to the $1\,^1S\rightarrow 2\,^1S$ excitation process in the presence of a laser field, in the case of a helium target, and for the absorption of one photon ($L=1$). The incident energy is $E_i=500$ eV, the laser photon energy is $\hbar\omega=1.17$ eV, and the electric field strength is $\mathcal{E}_0=10^6$ V cm^{-1}. The polarization vector of the field is taken to be parallel to the momentum transfer Δ. Solid line, full calculation using Eq. (16); dashed line, electronic result in which dressing effects are neglected.

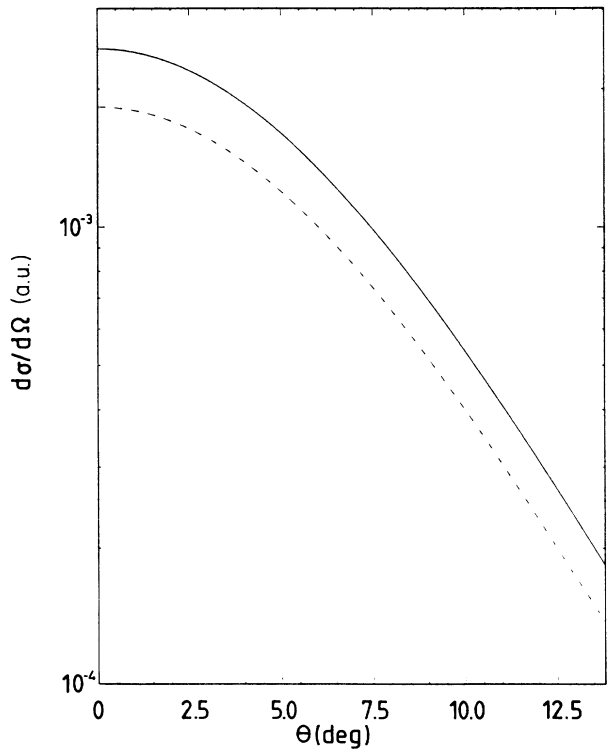

FIG. 8. Same as Fig. 7 but for the excitation of the $2\,^1P$ state of helium.

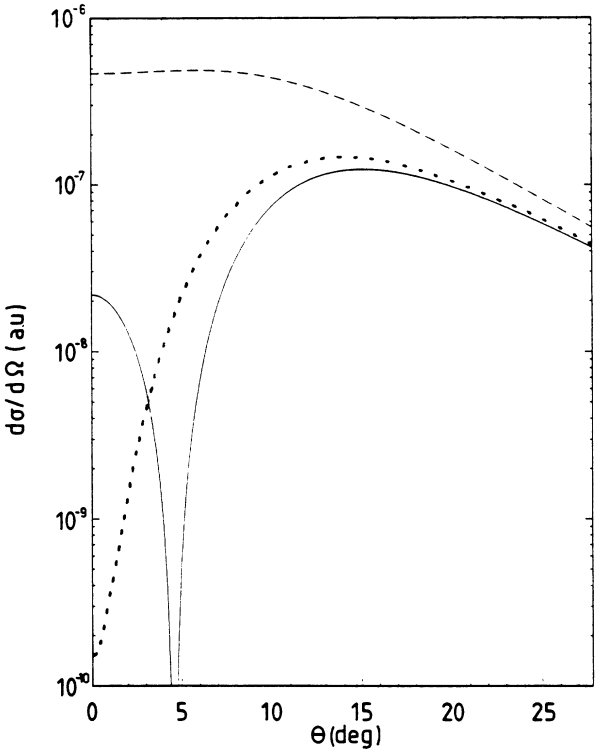

FIG. 9. Same as Fig. 7 but for the emission and the absorption of two photons ($L=\pm 2$). Solid line, full calculation in the case $L=2$; dashed line, full calculation in the case $L=-2$; dotted line, electronic result in the case $L=\pm 2$.

to that of a Nd:YAG laser, namely, $\hbar\omega=1.17$ eV. We stress that our conclusions would remain the same for other choices of those parameters.

The foregoing conclusions are further confirmed by the results given in Table IV. Here, the contribution (in percent) of the various intermediate states to the "atomic" amplitude is shown both in the case of $2\,^1S$ and $2\,^1P$ final states. As expected, the intermediate states with $n \leq 3$ always give the dominant contribution (about 90%). We note that, in the case of the $1\,^1S \rightarrow 2\,^1P$ process, we have chosen for the average excitation energy the value $\bar{\omega}_{2\,^1P}=\bar{\omega}_{2\,^1S}=0.218$ a.u. It should be noted that, albeit somewhat arbitrary, that choice has little incidence on the final results. We also notice that the results bear a close analogy with those obtained in atomic hydrogen.

In Fig. 7 we show the electronic and exact cross sections corresponding to the $1\,^1S \rightarrow 2\,^1S$ excitation process, in the case $L=1$ (absorption of one photon), as a function of the scattering angle θ. The other parameters are the same as in the tables. The behavior of the curves qualitatively agrees with what was obtained in the elastic case[3] and in atomic hydrogen. In particular, dressing effects are seen to be very large at small scattering angles, and a destructive interference between the electronic and atomic terms is clearly present. Figure 8 shows the corresponding results for the $1\,^1S \rightarrow 2\,^1P$ process. As expected, the importance of dressing effects is strongly reduced with respect to the preceding case. This is because the electronic amplitude now behaves like Δ^{-1} for small Δ, and is dominant at small Δ. As in the case of an atomic hydrogen target, the above-mentioned interference is also seen to be removed when considering S-P transitions. Finally, Fig. 9 shows the cross sections corresponding to the absorption and the emission of two photons ($L=\pm 2$), respectively. As discussed in detail above in the case of atomic hydrogen excitation, the theory predicts important asymmetries between inverse and stimulated bremsstrahlung. That feature constitutes one of the main differences between elastic and inelastic scattering in a laser field.

IV. CONCLUSION

In this work we have extended our analysis of electron-atomic hydrogen and electron-helium collisions in a laser field to the case of inelastic collisions. In the case of S-S and S-D transitions, dressing effects have been shown to be responsible for very important modifications of the cross sections at small scattering angles in the case of laser-assisted scattering. On the other hand, those effects are reduced drastically when considering S-P transitions. The frequency dependence of the various cross sections also presents new aspects because of possible intermediate resonances in the laser-atom interaction during the collision event. The presence of those resonances imposes new limitations to our approach, since for small detunings the domain of validity of our perturbative treatment is restricted to smaller

TABLE IV. Contribution (in percent) of the various intermediate states to the dressing term in Eq. (16), for the excitation of the $2\,^1S$ and $2\,^1P$ states of helium with the absorption of one photon ($L=1$) and for three values of the scattering angle θ. The incident electron energy, the laser photon energy, and the electric field strength are chosen as in Figs. 7 and 8.

	$1\,^1S \rightarrow 2\,^1S$				$1\,^1S \rightarrow 2\,^1P$		
	Intermediate state						
θ (deg)	$2\,^1P$	$3\,^1P$	$\sum_n n\,^1P$	$1\,^1S$	$2\,^1S$	$3\,^1S$	$3\,^1D$
0	83.44	6.58	99.87	0.64	91.75	1.47	6.11
5	82.38	6.75	99.81	0.74	92.32	1.58	5.35
10	80.20	6.96	99.60	1.10	93.33	1.72	3.78

values of the electric field strength than for elastic scattering. Nevertheless, this should constitute a "plus" from the experimentalist's point of view since it could allow the observation of dressing effects at lower laser intensities than in the elastic case, provided the laser frequency is chosen adequately.

ACKNOWLEDGMENTS

It is a pleasure to thank Professor A. Maquet for sending us the results of Ref. 6 prior to publication. One of us (P.F.) is supported by the IRSIA Institute.

APPENDIX A: EVALUATION OF THE CONTRIBUTION OF DOUBLY EXCITED STATES

The method we have used for evaluating the contribution of doubly excited states in the case of the $1\,^1S \rightarrow 2\,^1S$ process is the following. In a first step, let us consider Eq. (7) and make the closure approximation. The sums to be evaluated are of the form

$$S_1 \equiv \sum_{n'} M_{n',1\,^1S} f^{\mathrm{B1}}_{2\,^1S,n'}(\boldsymbol{\Delta}) = \sum_{n'} M_{2\,^1S,n'} f^{\mathrm{B1}}_{n',1\,^1S}(\boldsymbol{\Delta}) , \tag{A1}$$

and we obtain, in the same way as in Eq. (16),

$$S_1 = -2i\Delta^{-2}\mathcal{E}_0\cdot\nabla_\Delta \langle \psi_{2\,^1S}(r_1,r_2) \mid e^{i\boldsymbol{\Delta}\cdot\mathbf{r}_1} + e^{i\boldsymbol{\Delta}\cdot\mathbf{r}_2} - 2 \mid \psi_{1\,^1S}(r_1,r_2)\rangle . \tag{A2}$$

This expression is readily evaluated using the wave functions (17) and (19). It should be noted that the summation has been performed over all excited states, including doubly excited ones.

In a second step we use as intermediate states wave functions of the form (22). As discussed in Sec. II C, these describe only *simply* excited P states of helium. They enable us to evaluate the expression

$$S_2 = \sum_{n'}{}' M_{n',1\,^1S} f^{\mathrm{B1}}_{2\,^1S,n'}(\boldsymbol{\Delta}) = \sum_{n'}{}' M_{2\,^1S,n'} f^{\mathrm{B1}}_{n',1\,^1S}(\boldsymbol{\Delta}) , \tag{A3}$$

where the notation $\sum'$ means that the summation involves only simply excited states. Using Eqs. (17) and (19), Eq. (A3) reduces to

$$S_2 = -4C\Delta^{-2}\langle u_1(r_2) \mid \phi_0(r_2)\rangle \sum_{n,p,m} \langle \psi_{npm}(Z_0,r_1) \mid e\mathcal{E}_0\cdot\mathbf{r}_1 \mid \phi_0(r_1)\rangle \times [\langle u_2(r_1) \mid e^{i\boldsymbol{\Delta}\cdot\mathbf{r}_1} \mid \psi_{npm}(Z_0,\mathbf{r}_1)\rangle - \langle u_2(r_2) \mid u_1(r_2)\rangle\langle u_1(r_1) \mid e^{i\boldsymbol{\Delta}\cdot\mathbf{r}_1} \mid \psi_{npm}(Z_0,\mathbf{r}_1)\rangle] . \tag{A4}$$

Since the hydrogenic wave functions $\psi_{npm}(Z_0,\mathbf{r}_1)$ in turn form a complete set, closure can be used with respect to the variable $\mathbf{r}_1$ to yield the expression

$$S_2 = 4iC\Delta^{-2}\langle u_1(r) \mid \phi_0(r)\rangle \mathcal{E}_0\cdot\nabla_\Delta [\langle u_2(r) \mid e^{i\boldsymbol{\Delta}\cdot\mathbf{r}} \mid \phi_0(r)\rangle + \langle u_2(r) \mid u_1(r)\rangle\langle u_1(r) \mid e^{i\boldsymbol{\Delta}\cdot\mathbf{r}} \mid \phi_0(r)\rangle] , \tag{A5}$$

which can be evaluated in a straightforward way. Upon comparison between the results (A2) and (A5), the contribution of doubly excited states to the sum S_1 is then readily seen to be given by

$$S = S_1 - S_2 = 1024iCMN\mathcal{E}_0\Delta^{-1}\left[\frac{A}{(\alpha+2)^3}+\frac{B}{(\beta+2)^3}\right] \times \left[\frac{1}{(2+\tau_1)^2}-\frac{3S}{(2+\tau_2)^3}\right] \times \left[\frac{A(\alpha+2)}{[(\alpha+2)^2+\Delta^2]^3}+\frac{B(\beta+2)}{[(\beta+2)^2+\Delta^2]^3}\right] . \tag{A6}$$

APPENDIX B: WEAK-FIELD LIMIT OF EQ. (7)

1. Case $L > 0$ (absorption)

To lowest order in the external field $\mathcal{E}_0$ we can approximate the Bessel functions in Eq. (7) as

$$J_L(x) \simeq \frac{1}{L!}\left[\frac{x}{2}\right]^L \tag{B1}$$

and

$$J'_L(x) \simeq \frac{LJ_L(x)}{x} \simeq \frac{x^{L-1}}{(L-1)!2^L} , \tag{B2}$$

where $x = \boldsymbol{\Delta}\cdot\boldsymbol{\alpha}_0$. In that limit, Eq. (7) reduces to the simpler expression

$$f_{f,0}^{\mathrm{B1},L}=\frac{1}{L!}(\tfrac{1}{2}\Delta\cdot\alpha_0)^L f_{f,0}^{\mathrm{B1}}(\Delta) - \frac{i}{(L-1)!2^L}(\Delta\cdot\alpha_0)^{L-1}\left[\sum_{n'}\frac{M_{f,n'}}{\omega_{n',f}+\omega}f_{n',0}^{\mathrm{B1}}(\Delta) + \sum_{n'}\frac{M_{n',0}}{\omega_{n',0}-\omega}f_{f,n'}^{\mathrm{B1}}(\Delta)\right]. \tag{B3}$$

As a result, the first term in the large parentheses, in which the radiative transition connects the final state with an intermediate state n', cannot be resonant except if the intermediate state has a lower energy than the final state. We want to stress that the situation would be quite different at intermediate field strengths, since in this case resonant terms proportional to $J_L'(x)$ and $Lx^{-1}J_L(x)$ would not cancel any more.

2. Case $L<0$ (emission)

In this case, the formulas (B1) and (B2) become, respectively,

$$J_L(x)\simeq\frac{(-1)^L}{(-L)!}\left[\frac{x}{2}\right]^{-L} \tag{B4}$$

and

$$J_L'(x)\simeq -L\frac{J_L(x)}{x}\simeq\frac{(-1)^L}{(-L-1)!}\frac{x^{-L-1}}{2^{-L}} \tag{B5}$$

so that Eq. (7) now reduces to

$$f_{f,0}^{\mathrm{B1},L}=\frac{(-1)^L}{(-L)!}(\tfrac{1}{2}\Delta\cdot\alpha_0)^{-L}f_{f,0}^{\mathrm{B1}}(\Delta) - \frac{(-1)^L i}{(-L-1)!2^{-L}}(\Delta\cdot\alpha_0)^{-L-1}\times\left[\sum_{n'}\frac{M_{f,n'}}{\omega_{n',f}-\omega}f_{n',0}^{\mathrm{B1}}(\Delta) + \sum_{n'}\frac{M_{n',0}}{\omega_{n',0}+\omega}f_{f,n'}^{\mathrm{B1}}(\Delta)\right]. \tag{B6}$$

As a result, the situation is seen to be opposite to the case of absorption. Indeed, the first term in the large parentheses now becomes resonant for $\omega_{n'}>\omega_f$, while in the last term radiative $1S\rightarrow nP$ transitions become nonresonant.

[1] F. W. Byron, Jr. and C. J. Joachain, J. Phys. B **17**, L295 (1984).
[2] P. Francken and C. J. Joachain, Phys. Rev. A **35**, 1590 (1987).
[3] F. W. Byron, Jr., P. Francken, and C. J. Joachain, J. Phys. B **20**, 5487 (1987).
[4] N. K. Rahman and F. H. M. Faisal, J. Phys. B **11**, 2003 (1978).
[5] S. Jetzke, F. H. M. Faisal, R. Hippler, and O. H. Lutz, Z. Phys. A **315**, 271 (1984).
[6] S. Jetzke, J. Broad, and A. Maquet, J. Phys. B **20**, 2887 (1987).
[7] R. S. Pundir and K. C. Mathur, Z. Phys. D **1**, 385 (1986).
[8] I. I. Sobelman, *Introduction to the Theory of Atomic Spectra* (Pergamon, New York, 1972), p. 272.
[9] I. S. Gradshteyn and I. M. Ryzhik, *Table of Integrals, Series and Products* (Academic, New York, 1965), p. 966.
[10] F. W. Byron, Jr. and C. J. Joachain, Phys. Rev. **146**, 1 (1966).
[11] F. W. Byron, Jr. and C. J. Joachain, J. Phys. B **8**, L284 (1975).